HHS Public Access

Author manuscript

Transplantation. Author manuscript; available in PMC 2020 April 01.

Published in final edited form as:

Transplantation. 2019 April ; 103(4): 705–715. doi:10.1097/TP.0000000000002495.

mTOR Inhibitor Everolimus in Regulatory T cell Expansion for Clinical Application in Transplantation

Roberto Gedaly, MD[#1,*], **Felice De Stefano, MD**[1], **Lilia Turcios, PhD**[1], **Marita Hill**[2], **Giovanna Hidalgo**[2], **Mihail I. Mitov, PhD**[3,5], **Michael C. Alstott, MS**[3], **D. Allan Butterfield, PhD**[3,4], **Hunter C. Mitchell**[1,6], **Jeremy Hart, MD**[2], **Ahmad Al-Attar, MD**[2], **Chester D. Jennings, MD**[2], and **Francesc Marti, PhD**[#1,*]

[1]Department of Surgery - Transplant Division; University of Kentucky, College of Medicine, Lexington, KY 40536, U.S.A

[2]Department of Pathology and Laboratory Medicine; University of Kentucky, College of Medicine, Lexington, KY 40536, U.S.A

[3]Redox Metabolism (RM) Shared Resource Facility (SRF), Markey Cancer Center; University of Kentucky, College of Medicine, Lexington, KY 40536, U.S.A

[4]Department of Chemistry; University of Kentucky, College of Medicine, Lexington, KY 40536, U.S.A

[5]Idaho College of Osteopathic Medicine (ICOM), Meridian, ID 83642, U.S.A. (current address)

[6]Department of Science & Health, Asbury University, School of Science, Health & Mathematics, Wilmore KY 40390, U.S.A

[#] These authors contributed equally to this work.

Abstract

Background: Experimental and pre-clinical evidence suggest that adoptive transfer of regulatory T cells (Tregs) could be an appropriate therapeutic strategy to induce tolerance and improve graft survival in transplanted patients. The University of Kentucky Transplant Service Line is developing a novel Phase I/II clinical trial with *ex vivo* expanded autologous Tregs as an adoptive cellular therapy in renal transplant recipients who are using everolimus (EVR)-based immunosuppressive regimen.

[*]Corresponding Authors: Roberto Gedaly, MD and Francesc Marti, PhD, University of Kentucky Transplant Center, 740 South Limestone, K301, Lexington, KY, 40536-0284, USA, rgeda2@uky.edu & fmart3@uky.edu, Tel: 1-859-323-4661, FAX: 1-859-257-3644.

Authorship:
Designed research: RG and FM
Collected data: FDS, LT, GH, MIM, MCA, HCM and FM
Contributed analytic tools: MH, DAB, JH, CDJ
Analyzed data: RG, AAT and FM
Wrote the manuscript: RG and FM
Critical editing of content: all authors
Approval of final version: all authors

Disclosure: The authors declare no commercial or financial conflicts of interest

Clinical Trial Notation: National Cancer Trial Registry; # NCT03284242

Methods: The aim of this study was to determine the mechanisms of action and efficacy of EVR for the development of functionally competent Treg cell-based adoptive immunotherapy in transplantation to integrate a common EVR-based regimen *in vivo* (in the patient) and *ex vivo* (in the expansion of autologous Treg cells). CD25+ Treg cells were selected from leukapheresis product with a GMP-compliant cell separation system and placed in 5-day (short) or 21-day (long) culture with EVR or rapamycin (RAPA). Multi-parametric flow cytometry analyses were used to monitor the expansion rates, phenotype, autophagic flux and suppressor function of the cells. PI3K/AKT/mTOR signaling pathway profiles of treated cells were analyzed by western blot and cell bioenergetic parameters by extracellular flux analysis.

Results: EVR-treated cells showed temporary slower growth, lower metabolic rates, and reduced phosphorylation of AKT compared to RAPA-treated cells. In spite of these differences, the expansion rates, phenotype, and suppressor function of long-term Treg cells in culture with EVR were similar to those with RAPA.

Conclusions: Our results support the feasibility of EVR to expand functionally competent Treg cells for their clinical use.

INTRODUCTION

Organ transplantation is the treatment of choice for patients with advanced chronic or end-stage organ failure. The introduction and continued advances in immunosuppressive regimens during the last decades have led to a dramatic improvement in allotransplant survival rates. However, long-term use of powerful nonspecific immunosuppressants such as calcineurin inhibitors (CNIs) may cause adverse effects often linked with systemic toxicity, in particular nephrotoxicity, and may not properly control chronic immune-mediated allograft rejection[1,2]. The CNIs tacrolimus and cyclosporine A (CsA) are currently employed as the first line of therapeutic regimens in solid organ transplantation. Everolimus (EVR) is an immunosuppressive agent derivative of rapamycin (RAPA). RAPA works as a specific inhibitor of the mammalian target of RAPA (mTOR) when it is a member of the mTOR complex 1 (mTORC1), but not when it is part of the complex 2.[3] EVR has been approved by the FDA for heart, renal, and liver transplantation[4–6], and it can be used alone or in combination with CNIs to reduce CNI-induced toxicity.[7,8] In either case, the administration of EVR has been associated with a significant improvement in renal function and overall toxicity after transplant.[9–12]

Aside from pharmacologic drugs, biologic immunosuppressants have been gaining interest for their enormous clinical potential in sustaining graft acceptance. CD4+CD25hiFoxP3+ regulatory T cells (Tregs) constitute a small fraction of T cells (approximately 1–5% of circulating CD4+ T cells) that harbor immunosuppressive function and play a critical role in the induction and maintenance of peripheral tolerance and immune homeostasis. [13] Tolerant transplant recipients show increased frequencies of Tregs[14] while acute rejection is associated with low levels of circulating Tregs.[15] Indeed, increasing evidence supports the balance between graft-reactive effector cells and graft-protective suppressor Tregs as a determining factor in long-term allograft survival.[16–18] The ability of Treg cells to inhibit the effector immune reactions that trigger graft rejection have been demonstrated in numerous pre-clinical studies, and Tregs have become attractive candidates for the development of

therapeutic strategies aimed at tolerance induction[19]. However, the low frequency of peripheral Tregs has become a major obstacle for their clinical application. The production of large numbers of clinical grade cells entails the *ex vivo* expansion of Tregs in GMP-compatible conditions. Addition of RAPA is of standard use in these protocols since the targeting of the mTOR pathway leads to a preferential or selective expansion of Tregs over conventional T cells (Tconv)[20–23] and the stability of FoxP3 expression after *in vivo* transfer.[24] In a recent study, we reported that the dual targeting of PI3K and mTOR is also inducing the preferential expansion of mouse and human Tregs, and the resulting cells are able to promote *in vivo* tolerance.[23] In the same study, we showed that dual PI3K/mTOR inhibitors and RAPA induced similar changes in the phenotype and function of cultured Treg cells, although both families of drugs exert their effects through distinct alterations in the signaling and metabolic profiles.. Our group has just initiated a Phase I/II clinical trial with autologous Treg immunotherapy in kidney transplant patients receiving EVR in the conditioning regimen (NCT03284242). Consequently, we wanted to address the option of integrating a common immunosuppressive EVR-based regimen, which includes the expansion of autologous Treg cells *ex vivo* and the administration of the same mTOR inhibitor to the patient. However, in contrast to RAPA, little information is available regarding the effects promoted by EVR in Treg cells. Earlier studies by our group and others demonstrated the critical sensitivity of Treg cell differentiation, expansion and function to mTOR pathway perturbations.[20–32] In such terms, the aim of this study was to determine the mechanisms of action and efficacy of EVR for the clinical grade expansion of functional Treg cells.

MATERIALS and METHODS

Ethical approval of studies and informed consent

All experimental protocols were approved by an Institutional Review Board Committee at the University of Kentucky (16–0779-F6A). Peripheral blood mononuclear cells (PBMCs) were collected by leukapheresis from healthy donors (n=2) after obtaining written informed consent, or isolated from buffy coats of anonymous healthy donors (n=4) provided by the Kentucky Blood Center (Lexington, KY).

Purification and activation of primary human T cells

PBMCs were conjugated for 10 minutes at 4^{o}C with the CliniMACS CD25 MicroBeads reagent (Miltenyi). CD25+ cells were isolated in the CliniMACS system (Miltenyi, program *Enrichment 3.2*) according to the manufacturer instructions. The sequential gating strategy to identify the viability and purity of Treg cells resulting from the CD25+-enrichment process is depicted in Supplemental Digital Content (SDC), Figure S1. Tconv were isolated from PBMCs by negative selection with the use of the human CD4+ T cell isolation kit (StemCell Technologies). For initial stimulation of cells, the enriched CD25+ Treg cell fraction was placed in culture in closed, gas permeable GMP cell expansion bags (Miltenyi) at a concentration of 10^6 cells/mL in TexMACS GMP medium (Miltenyi) supplemented with 2% autologous serum, MACS GMP ExpAct Treg kit (Miltenyi) at a bead-to-cell ratio of 2:1, and either RAPA (MACS GMP Rapamycin, 100nM) or EVR (Selleckchem Chemicals, 100nM). After 48 hours, recombinant human IL-2 (MACS GMP hrIL2, 500 IU/mL) was added. At day 5, a sample from each condition was collected for short-term

analysis and the remaining cells were restimulated with ExpAct Treg beads, IL-2, and RAPA or EVR at a concentration of 10^6/mL. Cell growth was monitored throughout the remaining of the expansion process to maintain the cell density below 2×10^6 cells/mL.

Cell surface and intracellular staining, western blot analysis, metabolic characterization, mitochondrial and autophagy changes and methylation of the TSDR region of the *FOXP3* locus were assessed as previously described23,25 and detailed in SDC, Materials and Methods.

Statistics

Data are reported as mean±SD except where indicated. Experiments were performed at least in triplicate. Statistical significance of differences was analyzed using Kruskal–Wallis ANOVA followed by Wilcoxon's rank sum test for pairwise comparisons. Statistical analyses were performed using GraphPad PRISM 7.0. In all analyses, $p< 0.05$ was considered a statistically significant difference.

RESULTS

Isolation and culture of $CD4^+CD25^+$ Treg population

The phenotypic analysis of the CD25+-enriched fraction showed a mean CD4+ T cell purity (±SEM) of 96.7% (±2.8), and a CD25+/FoxP3+/CD127Low/- purity of 82.3% (±4.6) with cell viability consistently above 98% (Figure S1). Since the mTOR inhibitor EVR was not previously described as used for the culture of Tregs, we first assessed the optimal concentration of EVR needed for limiting the expansion of Tconv and increasing the population of CD25+-enriched Treg cells. After 5-day culture, the optimal concentration of EVR that resulted in the highest Treg and lowest Tconv expansion rates was determined to be 100nM (Figure S2). Accordingly, we set this as the default concentration of EVR to culture CD4+CD25+ Treg-enriched cells throughout the study. All parameters were compared with the effects induced by RAPA (100nM), the most widely used mTOR inhibitor to selectively prevent the outgrowth of contaminating Tconv in the *in vitro* culture of Tregs.[19–24]

Regulation of mTOR signaling pathway

Western blot analyses were performed on lysates of Treg cells cultured in expansion medium during 5 days alone or with the addition of EVR or RAPA. Figure 1 shows the significant decrease in the expression of phosphorylated p70S6k and 4EBP1, two of the major downstream substrates of mTORC1, the canonical target of rapalogs, in EVR- and in RAPA-treated cells compared to the 100% baseline expression of untreated control cells. The mTORC1 signaling attenuation occurred with the simultaneous increase of mTORC2 activity, as measured by the phosphorylation of AKT on Ser-473. This over-activation was less prominent in EVR (217.7%±16.1) than in RAPA-treated cells (372.1%±33.8). In addition, a substantial increase in phospho-ERK levels was also noted in response to both drug treatments (151.2%±4.6 and 156.0%±4.1, respectively). While the total expression of ERK was also reduced in drug-treated cells, AKT expression persisted in RAPA-treated cells. In contrast, EVR treatment promoted a significant reduction in AKT expression

(75.8%±5.5). The (phosphorylated / total) protein expression indexes (Figure S3) revealed that, in addition to the regulation of total protein expression, RAPA and EVR differently regulate the phosphorylation of AKT (higher in RAPA-treated cells) and 4EBP1 (higher in EVR-treated cells). In contrast, most of the differences observed in the expression levels of phospho-p70S6k derived from the regulation of total protein expression. Overall, our findings revealed distinct mTORC1/mTORC2 balances induced by RAPA and EVR in 5-day cultured Treg cells.

Treg cell bioenergetics

Treg cells rely preferentially in the mitochondrial oxidation of lipids or glucose to meet cell energy demands, although the glycolytic pathway seems to be also active during *in vitro* expansion.[32–35] In an early study, we reported the distinct bioenergetic profiles induced by RAPA and dual PI3K-mTOR inhibitors in Treg cells.[23] Following the same experimental approach, we evaluated whether the presence of EVR or RAPA may alter the cellular metabolism in expanding CD25+-enriched Treg cells. The OCR (an indirect measurement of oxidative phosphorylation -OxPhos-) and ECAR (an indicator of glycolytic flux) bioenergetic profiles were measured in 5-day cultured Treg cells and compared with Tconv cells also grown for 5 days in the same expansion medium (Figures 2–3 and S4). EVR-treated cells exhibited reduced OxPhos across all data points relative to RAPA-treated cells, with lower baseline levels (22.2±1.8 and 30.9±3.5 pmol/min) and, after FCCP injection, attenuated maximal OCR (128.2±9.1 and 211.4±11.6 pmol/min) and the corresponding spare respiratory capacity (SRC) levels (106.0±8.7 and 180.8±11.2 pmol/min), although no differences were noted on the ATP-linked oxygen consumption rates (Figures 2A-D). Addition of the irreversible inhibitor of carnitine palmitoyltransferase-1 (CPT-1), etomoxir, enables the evaluation of the relative contribution of endogenous fatty acid (FA) oxidation (FAO) to OxPhos. We found lower FA-dependent (70.4±5.3 pmol/min) and FA-independent OCR (57.9±4.4) in EVR relative to RAPA-treated cells (123.6±9.8 and 87.8±2.7 pmol/min, respectively). Unlike RAPA-treated cells, only FAO (but not FA-independent oxidation) was significantly augmented in EVR-treated cells compared to Tconv (37.7±8.2 pmol/min for FAO, and 55.1±4.5 for FA-independent respiration). The FAO index (FA-dependent / FA independent) >1 in all Treg conditions (untreated and EVR- or RAPA-treated) illustrates the preferential use of FA as OxPhos substrate. In contrast, the low OxPhos rates in Tconv cells were mostly driven by non-FA (etomoxir-resistant) substrates. In separate ECAR experiments, addition of RAPA or EVR reduced the glycolytic profile, which may account for the observed lower expansion rates of treated compared to untreated Treg cells. When compared both drugs, EVR treatment resulted in lower ECAR baseline levels (5.9±0.6 mpH/min) and in response to glucose (26.1±3.0) than RAPA (7.5±0.7 and 30.70±3.2 mpH/min) (Figures 3A-C). However, the glycolytic capacity (as measured upon injection of the OxPhos inhibitor oligomycin) and the glycolytic reserve (that represents the difference between glycolytic capacity and glycolysis rate) did not differ between both treatments (42.8±7.2 vs 50.3±4.7 mpH/min and 16.7±4.3 vs 19.7±1.7 mpH/min, respectively) (Figures 3D-E). As expected by their strong dependency on glycolysis, cultured Tconv displayed a sharp increase in the glycolytic rate after the addition of exogenous glucose (54.8±3.0 mpH/min) but a limited capacity to respond to oligomycin (7.3±3.1 mpH/min). Similarly, addition of oligomycin promoted a significant increase in the ECAR values recorded on the OCR

experiments in RAPA- and EVR-treated cells (61.9%±4.5 and 48.4%±5.5, respectively) (Figure S5-A). In contrast, ECAR levels in Tconv cells remain largely unresponsive to oligomycin. The plot of OCR vs ECAR under basal conditions and under maximal OCR and glycolytic flux (Figure S4-A) illustrates the different bioenergetic profiles and relative utilization of OxPhos and glycolysis of expanding Tregs and Tconv cells, and revealed the reduced cell metabolism of 5 day-EVR-treated cells relative to RAPA. The OCR/ECAR rates (Figures S4-B-C) confirmed the high glycolytic dependency of proliferating Tconv and the predominant OxPhos energy profiles of Treg cells. Worth noting also is that both RAPA and EVR treatments promoted the reliance of expanding Treg cells on mitochondrial respiration.

Mitochondrial morphology and function

The different OxPhos activity promoted by EVR and RAPA in Treg cells may associate with changes in mitochondrial membrane potential ($\Delta\Psi m$), a critical parameter of mitochondrial functional integrity. To address this possibility, we measured $\Delta\Psi m$ with the TMRE fluorescent dye in 5 day-expanded untreated (control) and drug-treated cells. The reliability of the TMRE uptake to measure $\Delta\Psi m$ was confirmed for each condition by the collapse of the $\Delta\Psi m$ upon pre-incubation with the decoupler proton ionophore FCCP. To rule out any biased result as a consequence of changes in mitochondrial mass, the TMRE loading results were normalized for mitochondrial content and were expressed as the ratios between TMRE and MitoTracker Green FM fluorencences as reported elsewhere.[35] The MitoTracker Green FM results revealed the increase in mitochondrial mass in RAPA-treated cells (447±45 MFI) compared to EVR (385±29 MFI,) and untreated cells (367±42 MFI). Once normalized, the $\Delta\Psi m$ results were not significantly different among different conditions (Figure 4A). Since the activation of the PI3K/mTOR pathway is known to negatively influence autophagy and RAPA is reportedly promoting autophagy in different cell settings[36,37], we next asked whether EVR induced similar effects in Treg cells. The analyses with the Cyto-ID Green detection reagent demonstrated that EVR also increased the formation of autophagosomal vacuoles (6288±427 MFI) compared to untreated control cells (5518±345). However, the vacuole formation in EVR samples was significantly lower than in RAPA samples (7245±222). Addition of CLQ to measure autophagic flux produced similar accumulation of autophagosomes in response to both drugs (2143±134 MFI for EVR and 2214± 68 for RAPA), both significantly higher than in the untreated group (1442±48) (Figure 4B).

Treg cell phenotype and regulatory activity

The presence of RAPA or EVR did not induce any significant phenotypic difference in the 5-day expanded cells. The mean fluorescent intensity (MFI) of CD25 and FoxP3 expression was similar under the two drug conditions, as well as the expression of other Treg-related cell markers including CTLA-4, CD49d (depicted in Figure S6), PD1, PDL-1, OX40, GITR and CD86 (data not shown). The functional properties of expanded Tregs in the presence of EVR or RAPA were assessed by their ability to suppress the proliferation of Tconv. The data demonstrated the equivalent suppressive function elicited by EVR- and RAPA-Tregs (Figure S7). The functional properties of expanded Tregs in the presence of EVR or RAPA were assessed by their ability to suppress the proliferation of Tconv. The data demonstrated the equivalent suppressive function elicited by EVR- and RAPA-Tregs (Figure S7).

Generation of clinical grade Treg cells

Manufacturing clinical grade cellular products for application in adoptive immunotherapy requires the *ex vivo* expansion of the original pool of cells. In order to validate the use of EVR to generate sufficient cell numbers of high-quality, clinical-grade Treg cells, freshly isolated CD4+CD25+ cells were expanded in the absence or in the- presence of EVR (100nM) or RAPA (100nM). Addition of EVR or RAPA promoted similar cell growth rates (Figures 5A-B), although the cells in EVR-medium experienced a temporary delay in early stages of culture (Figure S8). In the absence of rapalogs, the long-term expansion produced significantly larger cell yields (Figure 5B). However, these cells displayed a reduced suppressor activity when compared to drug-treated cells, while no significant differences in suppressive capacity were noted between both rapalog treatments (Figure 5C). The demethylation of the CpG dinucleotides at the highly conserved TSDR region of the *FOXP3* locus is necessary for Treg cell lineage stability[38]. Both RAPA- and EVR-treated cells show low expression of methylation levels across the nine CpG sites of the TSDR (ranges between 5.9 and 12.1% and 6.2 to 13.1%, respectively, in 6 samples), while the untreated cells displayed a broader range of methylation (between 12.3 and 43.6%, n=6) (Figure 5D). The same treatments in conventional T cells produce methylation levels at the TSDR CpG sites ranging from 81 to 97% (n=8). The high purity of the initial CD4+CD25+ Treg cells was sustained along the 21-day *ex vivo* expansion period in both RAPA- and EVR-treated cells. The absence of rapalogs in the expansion cell culture produced a final population with inconsistent contamination of CD8+ T cells (ranging from less than 3% to 27% of total T cells in 6 experiments) and with a population of CD4+CD25+ displaying lower expression of FoxP3 and CD25 markers compared to EVR- or RAPA-treated cells (Figure 6A). Further phenotype analysis of these cells showed also a different profile of several phenotype markers expressed distinctly in Tregs and Tconv cells (Figure S9), including higher intracellular IL-10, Helios, CCR4, CTLA4 and CD36, and lower expression of TIGIT and PD1 in rapalog-treated cells (Figure 6B), while no substantial differences were noted between RAPA and EVR cell culture phenotypes. The functional and phenotypic similarities between long-term expanded drug-treated cells also concur with the convergence of the oxidative metabolism (Figure 7) and glycolytic rates (Figure S5-B) in EVR- and RAPA-treated Tregs which, coincidently, displayed equivalent measurements in mitochondrial mass, $m\Delta\psi$ and autophagy (not shown),

DISCUSSION

The allosteric mTOR inhibitors RAPA and EVR are increasingly used in transplantation to minimize the dosage of CNIs in an attempt to reduce the risk of nephrotoxicity and incidence of malignancy.[39–41] Comparative pharmacokinetics suggest that EVR exhibits greater intestinal absorption compared to RAPA.[42] The relative hydrophobicity of RAPA makes it readily absorbed through the skin and is used in custom topical preparations.[43] In contrast, RAPA systemic clearance is half that of EVR44,45, which allows for EVR to reach faster steady state levels after the initiation of treatment and faster elimination after withdrawal. To date, there are no clinical trials directly comparing EVR and RAPA in cancer therapy or transplant, and there is limited literature on the characterization of the effects induced by EVR on T cells. A comparative study by Roat et al.46 among liver transplant

patients under CsA or EVR revealed that patients taking EVR had a higher percentage of total and naïve $CD4^+$ T cells than those treated with CsA, a lower percentage and functional response of $CD8^+$ T cells, and a higher percentage of Tregs. Levistky et al.47 reported a significant amplification of newly generated and natural Tregs in a mixed lymphocyte culture with EVR compared with mycophelonate, RAPA, and tacrolimus. Huijts et al.[26] showed that mTOR inhibition by RAPA or EVR increased the immunosuppressive capacity of the total Treg cell enriched population caused by the increased frequency of Tregs but not by the alteration of the suppressive activity per cell.

Here we confirmed the advantage of adding rapalogs for the *ex vivo* expansion of functional, clinical grade Treg cells and performed a comparative assessment of mechanisms of action and efficacy of EVR and RAPA. Our results demonstrated a similar efficacy of EVR and RAPA to expand functional Treg cells, although EVR treatment showed an early delay in cell growth (Figure S8). During this early phase, both drugs reduced the glycolytic rates in Treg cells, but only RAPA enhanced the mitochondrial OxPhos activity compared to untreated cells (Figures 2 and 3). The oligomycin-induced inhibition of OxPhos activity resulted in the rapid metabolic shift from OxPhos to aerobic glycolysis (Figure S5), which was further corroborated in separate ECAR experiments (Figure 3E). This oligomycin-dependent increase in glycolytic rates illustrates the metabolic plasticity of Treg cells previously suggested by Procaccini et al.[35] and is consistent with the ability of expanding Tregs to use glucose as a substrate for both mitochondrial respiration and aerobic glycolysis[33,34] even in long-term expanded Treg cells (Figure S4-B). In contrast, the glycolytic rates remained steady in Tconv upon mitochondrial OxPhos inhibition. The robust SRC and high glycolytic reserve levels in proliferating Tregs add further evidence of the cells' metabolic adaptability to sustain their intracellular ATP demand. This bioenergetic plasticity may allow Tregs to experience temporary metabolic stress without triggering cell death in a similar way as reported in some cancer cells.[48] Our results also revealed qualitative differences between Tregs and Tconv in OxPhos substrate utilization, as reflected by the major contribution of FA in Tregs and non-FA in Tconv. The inability of Tconv cells to oxidize glucose suggests the use of alternative non-FA, likely amino-acids49–50, as preferential mitochondrial substrates. In the context of the *ex vivo* expansion of Tregs, with the cells growing under conditions of unlimited nutrient availability, RAPA-treated cells appear to exhibit more active metabolism than EVR-treated cells during the early culture phase, which may account for their faster cell expansion growth seen in our study. As suggested for CD8+ memory T cells[49], the increase in mitochondrial mass (Figure 4A) may contribute to the higher oxidative and glycolytic capacity of RAPA-treated Tregs.

The differences between EVR and RAPA in the regulation of the Treg metabolic responses were associated with a different pattern of mTOR signaling activation. Both drugs produced similar attenuation on the phosphorylation of 4EBP1 and p70S6k, two main downstream effectors of mTORC1, as well as similar compensatory over-activation of ERK. However, the balance between mTORC1 and mTORC2 activities was differently perturbed; although both treatments increased the expression levels of mTORC2-dependent phosphorylation of AKT in Ser-473 when compared to untreated control cells, the increment was significantly lower in EVR-treated cells. The reduced total AKT expression in EVR-treated cells is likely contributing to the partial over-activation of AKT. However, we cannot discard the

participation of different feedback loops and/or compensatory mechanisms within the complex PI3K/AKT/mTOR signaling cluster.[27] Since the activation of mTORC2-dependent AKT is a critical marker for increased glycolysis in T cells[51] and in agreement with the mTORC2 necessary role in cell growth, proliferation and survival[28–30], we can rationally speculate a functional link between the weaker activation of AKT, the reduced glycolytic phenotype, and the slower proliferative rates in the early stages of EVR-treated Treg cell culture. In contrast, the suppressive function or the phenotypic profile of expanding Treg cells were independent of this metabolic and signaling fluctuations, which is consistent with the different molecular circuitries that regulate expansion and suppressor activity in *de novo* differentiated FoxP3+ Treg cells described in a previous study.[25] This possibility is also in line with the direct regulation of the suppressive function of Tregs by mTORC1.[31,32]

The increased activity of mTORC1 is generally perceived as a potent inhibitor of autophagy[52] and, consequently, the mTORC1-inhibitor RAPA is widely employed to induce autophagy[37]. Consistent with the same mTORC1 inhibitory capacity of RAPA and EVR in Treg cells, both drugs induced similar increase of autophagic flux. A potential cause for the increased autophagosome formation in RAPA-treated Tregs may rely on their high mitochondrial mass.[53,54] The combination of high autophagosome formation and mitochondrial mass raised the possibility of autophagic stress in RAPA-treated cells. However, long-term cell viability, expansion, phenotype and function did not differ between EVR and RAPA treatments, suggesting that the differences in autophagy processes did not exceed a threshold value to elicit any measurable damaging effect in the cell. In this context, the metabolic plasticity of Treg cells and their ability to redirect the energy metabolism towards glycolysis may also contribute to minimizing the potential damage associated with high mitochondrial OxPhos activity.[55]. Additional evidence against the likelihood of autophagy stress induction in RAPA-treated Treg cells was generated. First, we previously reported that autophagy-deficient Treg cells exhibit a significant decrease in $\Delta\Psi m$ as well as metabolic and functional deficits;[25] in contrast, none of these parameters were similarly altered in the current study after the exposure of Treg cells to RAPA. Importantly, the suppressor activity was consistently equivalent between both treatments throughout the *ex vivo* expansion process. Second, our findings suggest that the differences induced by EVR and RAPA in day 5 of the *ex vivo* culture are temporary, as evidenced by the subsequent expansion rates as well as the phenotypic, functional, and metabolic profile progressions of both cell treatments.

In the absence of EVR or RAPA, the expansion of Treg cells, even in our conditions of low activation, may produce a significant degree of contaminant CD8+ non-Treg cells. In addition, the fact that the expression levels of standard Treg markers such as CD25 and FoxP3 are low in untreated CD4+ T cells brings into question the degree of purity of these Tregs, further unsettled by the higher methylation status of the TSDR-*FOXP3* region. In the absence of Treg cell-specific membrane markers, the discrimination between effector and Treg cells for clinical use may be challenging. From the results generated in this study, we are currently analyzing the link between the different expression of TIGIT and CD36 in untreated and treated Treg cells and their functional capacities. On the other hand, the genomic location of *FOXP3* on the X chromosome should caution from a gender-biased expression. X chromosome inactivation (XCI) in female mammals generates a

transcriptionally silent inactive X chromosome (Xi) that, in case of FOXP3, remains highly methylated56–58. However, gender differences remain on the methylation status of the *FOXP3* gene even after corrected with a factor of 2. Although there is no evidence to date that *FOXP3* is among the immune-related genes that escape XCI in humans56,59, other gender-specific differences are arising with respect to the increased expression of FOXP3 in females, including androgen dependent sensitivity of FOXP3 expression[60] and the potential role of some functional FOXP3 variants61–66. These gender-specific epigenetic states and regulatory cues are likely to have important implications for understanding gender dimorphic variability of Treg cells in health and disease and strongly support the stratification of the Treg studies based on gender.

Similar to our pilot study (NCT03284242), the polyclonal Treg cell yield required in Plase I/II clinical trials is in the range of $1–10 \times 10^8$ cells. We choose to expand the cells in a rather low activation regimen (relative low dose of IL2 and bead concentration) to reduce the response of potential contaminating effector cells. Addition of rapamycin or EVR will further support this purpose while allowing an expansion rate of 80 times the original cell yield. From the initial leukapheresis product, we obtain a number of CD25+ Tregs ranging from 50 to 80×10^6, which allow us to reach (and exceed) the intended Treg cell number. In agreement with others,20–22 our results suggest that the absence of rapalogs in the expansion cell culture may represent a significant risk of contamination with unwanted non-Treg cells.

Our results also revealed the efficacy of *ex vivo* EVR Treg cell expansion and support EVR as a potential alternative to RAPA in the generation of clinical grade Treg cells. We reported several novel key findings regarding the distinct mechanisms of action of EVR in short-term cultured Treg cells, including the lower mTORC2 activity associated with an overall reduced metabolism and slow early expansion rates compared to RAPA. This initial EVR-Treg cell expansion delay, however, was overcome at later stages, and both RAPA and EVR treatments produced similar number of competent Treg cells with equivalent phenotype and functional suppressive activity. Overall, our findings support the implementation of a common immunosuppressive EVR-based regimen in the transplant patient that includes the adoptive infusion of *ex vivo* EVR-expanded autologous Treg cells.

Supplementary Material

Refer to Web version on PubMed Central for supplementary material.

Acknowledgments

Funding sources: This research was supported by the National Institute of Allergy and Infectious Diseases (NIAID) NIH grant R03-AI135592 to F.M., and by the National Center for Research Resources and the National Center for Advancing Translational Sciences, NIH grant UL1TR001998 to R.G. and F.M. The Redox Metabolism Shared Resource (RMSR) and the University of Kentucky Flow Cytometry and Immune Monitoring (FCIM) core facilities received support from the National Cancer Institute (NCI) NIH Cancer Center Support Grant P30CA177558 awarded to the University of Kentucky Markey Cancer Center. The content of this manuscript is solely the responsibility of the authors and does not necessarily represent the official views of the NIH.

Abbreviations:

4EBP1	eukaryotic translation initiation factor 4E-binding protein 1
AKT	protein kinase B
CD	cluster of differentiation
CFSE	carboxyfluorescein succinimidyl ester
CNIs	calcineurin inhibitors
CPT-1	carnitine palmitoyl-transferase
CsA	cyclosporine A
ECAR	extracellular acidification rates
ERK	extracellular signal-regulated kinase
EVR	everolimus
FA	fatty acid
FAO	fatty acid oxidation
FCCP	trifluorocarbonylcyanide phenylhydrazone
FoxP3	forkhead box P3
IL	interleukin
MFI	mean fluorescence intensity
mTOR	mammalian target of rapamycin
mTORC	mammalian target of rapamycin complex
OCR	oxygen consumption rate
OxPhos	mitochondrial oxidative phosphorylation
p70S6k	70 kDa ribosomal protein S6 kinase
PBMCs	peripheral blood mononuclear cells
PI3K	phosphoinositide 3-kinase
RAPA	rapamycin (sirolimus)
SD	standard deviation
SDC	supplemental digital content
SEM	standard error of the mean
SRC	spare respiratory capacity

Tconv	conventional T cells
Tregs	regulatory T cells
$\Delta\Psi m$	mitochondrial membrane potential

References

1. Elens L, Bouamar R, Shuker N, Hesselink DA, van Gelder T, van Schaik RH. Clinical implementation of pharmacogenetics in kidney transplantation: calcineurin inhibitors in the starting blocks. Br J Clin Pharmacol. 2014;77:715–28 [PubMed: 24118098]
2. Bamoulid J, Staeck O, Halleck F, et al. The need for minimization strategies: current problems of immunosuppression. Transpl Int. 2015;28:891–900. [PubMed: 25752992]
3. Ballou LM, Lin RZ. Rapamycin and mTOR kinase inhibitors. J Chem Biol. 2008;1:27–36. [PubMed: 19568796]
4. Budde K, Becker T, Arns W, et al. Everolimus-based, calcineurin-inhibitor-free regimen in recipients of de-novo kidney transplants: an openlabel, randomised, controlled trial. Lancet. 2011;377:837–47 [PubMed: 21334736]
5. Zuckermann A, Wang SS, Epailly E, et al. Everolimus immunosuppression in de novo heart transplant recipients: what does the evidence tell us now? Transplant Rev (Orlando). 2013;27:76–84. [PubMed: 23643624]
6. Yee ML, Tan HH. Use of Everolimus in Liver Transplantation. World J Hepatol. 2017;9:990–1000. [PubMed: 28878864]
7. Sterneck M, Kaiser GM, Heyne N, et al. Long-term follow-up of five yr shows superior renal function with everolimus plus early calcineurin inhibitor withdrawal in the PROTECT randomized liver transplantation study. Clin Transplant. 2016;30:741–8. [PubMed: 27160359]
8. Lin M, Mittal S, Sahebjam F, Rana A, Sood GK. Everolimus with early withdrawal or reduced-dose calcineurin inhibitors improves renal function in liver transplant recipients: A systematic review and meta-analysis. Clin Transplant. 2017;31:e12872.
9. Saliba F, De Simone P, Nevens F, et al. Renal function at two years in liver transplant patients receiving everolimus: results of a randomized, multicenter study. Am J Transplant. 2013;13:1734–45. [PubMed: 23714399]
10. De Simone P, Nevens F, De Carlis L, et al. Everolimus with reduced tacrolimus improves renal function in de novo liver transplant recipients: a randomized controlled trial. Am J Transplant. 2012;12:3008–20. [PubMed: 22882750]
11. Fischer L, Klempnauer J, Beckebaum S, et al. A randomized, controlled study to assess the conversion from calcineurin-inhibitors to everolimus after liver transplantation--PROTECT. Am J Transplant. 2012;12:1855–65. [PubMed: 22494671]
12. Fischer L, Saliba F, Kaiser GM, et al. Three-year Outcomes in De Novo Liver Transplant Patients Receiving Everolimus With Reduced Tacrolimus: Follow-Up Results From a Randomized, Multicenter Study. Transplantation. 2015;99:1455–62. [PubMed: 26151607]
13. Sakaguchi S, Yamaguchi T, Nomura T, Ono M. Regulatory T cells and immune tolerance. Cell. 2008;133:775–87. [PubMed: 18510923]
14. Li Y, Koshiba T, Yoshizawa A, et al. Analyses of peripheral blood mononuclear cells in operational tolerance after pediatric living donor liver transplantation. Am J Transplant. 2004; 4:2118–25. [PubMed: 15575917]
15. Demirkiran A, Kok A, Kwekkeboom J, et al. Low circulating regulatory T-cell levels after acute rejection in liver transplantation. Liver Transpl. 2006;12:277–84. [PubMed: 16447185]
16. Hanidziar D, Koulmanda M. Inflammation and the balance of Treg and Th17 cells in transplant rejection and tolerance. Curr Opin Organ Transplant. 2010;15:411–15. [PubMed: 20613526]
17. Wang Y, Zhang M, Liu ZW, et al. The ratio of circulating regulatory T cells (Tregs)/Th17 cells is associated with acute allograft rejection in liver transplantation. PLoS One. 2014;9:e112135. [PubMed: 25372875]

18. Teshima T, Maeda Y, Ozaki K. Regulatory T cells and IL-17-producing cells in graft-versus-host disease. Immunotherapy. 2011;3:833–52. [PubMed: 21751953]
19. Lam AJ, Hoeppli RE, Levings MK. Harnessing Advances in T Regulatory Cell Biology for Cellular Therapy in Transplantation. Transplantation. 2017;101:2277–87. [PubMed: 28376037]
20. Battaglia M, Stabilini A, Roncarolo MG. Rapamycin selectively expands CD4+ CD25+ FoxP3+ regulatory T cells. Blood. 2005;105:4743–48. [PubMed: 15746082]
21. Strauss L, Whiteside TL, Knights A, Bergmann C, Knuth A, Zippelius A. Selective survival of naturally occurring human CD4 + CD25 + Foxp3 + regulatory T cells cultured with rapamycin. J Immunol. 2007;178:320–9. [PubMed: 17182569]
22. Fraser H, Safinia N, Grageda N, et al. A Rapamycin-Based GMP-Compatible Process for the Isolation and Expansion of Regulatory T Cells for Clinical Trials. Mol Ther Methods Clin Dev. 2018;8:198–209 [PubMed: 29552576]
23. Vilchez V, Turcios L, Butterfield DA, et al. Evidence of the immunomodulatory role of dual PI3K/mTOR inhibitors in transplantation: an experimental study in mice. Transpl Int. 2017;30:1061–74. [PubMed: 28543637]
24. Tresoldi E, Dell'Albani I, Stabilini A, et al. Stability of human rapamycin-expanded CD4 + CD25 + T regulatory cells. Haematologica.2011;96:1357–65. [PubMed: 21565906]
25. Ellis GI, Zhi L, Akundi R, Büeler H, Marti F. Mitochondrial and cytosolic roles of PINK1 shape induced regulatory T-cell development and function. Eur J Immunol. 2013;43:3355–60. [PubMed: 24037540]
26. Huijts CM, Santegoets SJ, Quiles Del Rey M, et al. Differential effects of inhibitors of the PI3K/mTOR pathway on the expansion and functionality of regulatory T cells. Clin Immunol. 2016;168:47–54. [PubMed: 27189717]
27. Coquillard C, Vilchez V, Marti F, Gedaly R. mTOR Signaling in Regulatory T Cell Differentiation and Expansion. SOJ Immunol. 2015;3:1–10.
28. Zou Z, Chen J, Liu A, Zhou X, et al. mTORC2 promotes cell survival through c-Myc–dependent up-regulation of E2F1. J Cell Biol. 2015; 11:105–22.
29. Eltschinger S, Loewith R. TOR complexes and the maintenance of cellular homeostasis. Trends Cell Biol. 2016;26:148–59. [PubMed: 26546292]
30. Gaubitz C, Prouteau M, Kusmider B, et al. TORC2 structure and function. Trends Biochem Sci. 2016;41:532–45. [PubMed: 27161823]
31. Park Y, Jin HS, Lopez J, et al. TSC1 regulates the balance between effector and regulatory T cells. J Clin Invest. 2013;123:5165–78. [PubMed: 24270422]
32. Zeng H, Yang K, Cloer C, Neale G, Vogel P, Chi H. mTORC1 couples immune signals and metabolic programming to establish T(reg)-cell function. Nature. 2013;499:485–90. [PubMed: 23812589]
33. Gerriets VA, Kishton RJ, Nichols AG, et al. Metabolic programming and PDHK1 control CD4+ T cell subsets and inflammation. J Clin Invest. 2015;125:194–207. [PubMed: 25437876]
34. Michalek RD, Gerriets VA, Jacobs SR, et al. Cutting edge: distinct glycolytic and lipid oxidative metabolic programs are essential for effector and regulatory CD4+ T cell subsets. J Immunol. 2011;186:3299–3303. [PubMed: 21317389]
35. Procaccini C, Carbone F, Di Silvestre D, et al. The proteomic landscape of human ex vivo regulatory and conventional T cells reveals specific metabolic requirements. Immunity. 2016;44:406–42. [Published erratum appears in Immunity. 2016;44:712]. [PubMed: 26885861]
36. Claus C, Chey S, Heinrich S, et al. Involvement of p32 and microtubules in alteration of mitochondrial functions by rubella virus. J Virol. 2011;85:3881–92. [PubMed: 21248045]
37. Harder LM, Bunkenborg J, Andersen JS. Inducing autophagy: a comparative phosphoproteomic study of the cellular response to ammonia and rapamycin. Autophagy. 2014;10:339–55. [PubMed: 24300666]
38. Polansky JK, Kretschmer K, Freyer J, et al. DNA methylation controls Foxp3 gene expression. Eur J Immunol. 2008;38:1654–63. [PubMed: 18493985]
39. Sumethkul V, Tankee P, Worawichawong S, Jirasiritham S. Ten-Year Follow-up of Parmacokinetics-Guided Very Early Cyclosporine Minimization Synchronized With Everolimus

Initiation in De Novo Kidney Transplantation. Transplant Proc. 2017;49:1743–46. [PubMed: 28923619]

40. Yanik EL, Siddiqui K, Engels EA. Sirolimus effects on cancer incidence after kidney transplantation: a meta-analysis. Cancer Med. 2015;4:1448–59. [PubMed: 26108799]
41. Knoll GA, Kokolo MB, Mallick R, et al. Effect of sirolimus on malignancy and survival after kidney transplantation: systematic review and meta-analysis of individual patient data. BMJ. 2014;349:g667.
42. Lamoureux F, Picard N, Boussera B, Sauvage FL, Marquet P. Sirolimus and everolimus intestinal absorption and interaction with calcineurin inhibitors: a differential effect between cyclosporine and tacrolimus. Fundam Clin Pharmacol. 2012;26:463–72. [PubMed: 21631587]
43. Rauktys A, Lee N, Lee L, Dabora SL. Topical rapamycin inhibits tuberous sclerosis tumor growth in a nude mouse model. BMC Dermatol. 2008;8:1. [PubMed: 18226258]
44. Kirchner GI, Meier-Wiedenbach I, Manns MP. Clinical pharmacokinetics of everolimus. Clin Pharmacokinet. 2004;43:83–95. [PubMed: 14748618]
45. Moes DJ, Press RR, den Hartigh J, van der Straaten T, de Fijter JW, Guchelaar HJ. Population pharmacokinetics and pharmacogenetics of everolimus in renal transplant patients. Clin Pharmacokinet. 2012;51:467–80. [PubMed: 22624503]
46. Roat E, De Biasi S, Bertoncelli L, et al. Immunological advantages of everolimus versus cyclosporin A in liver-transplanted recipients, as revealed by polychromatic flow cytometry. Cytometry A. 2012;81:303–11. [PubMed: 22311717]
47. Levitsky J, Miller J, Huang X, Gallon L, Leventhal JR, Mathew JM. Immunoregulatory Effects of Everolimus on In Vitro Alloimmune Responses. PLoS One. 2016;8;11:e0156535.
48. Hao W, Chang C-PB, Tsao C-C, Xu J. Oligomycin-induced Bioenergetic Adaptation in Cancer Cells with Heterogeneous Bioenergetic Organization. J Biol Chem. 2010;285:12647–54. [PubMed: 20110356]
49. van der Windt GJ, Pearce EL. Metabolic switching and fuel choice during T-cell differentiation and memory development. Immunol Rev. 2012;249:27–42. [PubMed: 22889213]
50. Klysz D, Tai X, Robert PA, Craveiro M, et al. Glutamine-dependent α-ketoglutarate production regulates the balance between T helper 1 cell and regulatory T cell generation. Sci Signal. 2015;8:ra97. [PubMed: 26420908]
51. Wahl DR, Byersdorfer CA, Ferrara JL, Opipari AW, Jr, Glick GD. Distinct metabolic programs in activated T cells: opportunities for selective immunomodulation. Immunol Rev. 2012;249:104–15. [PubMed: 22889218]
52. Noda T, Ohsumi Y. Tor, a phosphatidylinositol kinase homologue, controls autophagy in yeast. J Biol Chem.1998;273:3963–66. [PubMed: 9461583]
53. Hailey DW, Rambold AS, Satpute-Krishnan P, et al. Mitochondria supply membranes for autophagosome biogenesis during starvation. Cell. 2010;141:656–67. [PubMed: 20478256]
54. Cook KL, Soto-Pantoja DR, Abu-Asab M, Clarke PA, Roberts DD, Clarke R. Mitochondria directly donate their membrane to form autophagosomes during a novel mechanism of parkin-associated mitophagy. Cell Biosci. 2014;4:16. [PubMed: 24669863]
55. Jeong DW, Kim TS, Cho IT, Kim IY. Modification of glycolysis affects cell sensitivity to apoptosis induced by oxidative stress and mediated by mitochondria. Biochem Biophys Res Commun. 2004;313:984–91. [PubMed: 14706639]
56. Carrel L, Willard HF. X-inactivation profile reveals extensive variability in X-linked gene expression in females. Nature. 2005;434:400–4. [PubMed: 15772666]
57. Fontenot JD, Rasmussen JP, Williams LM, Dooley JL, Farr AG, Rudensky AY. Regulatory T cell lineage specification by the forkhead transcription factor foxp3. Immunity. 2005;2:329–41.
58. Cottrell S, Jung K, Kristiansen G, Eltze E, et al. Discovery and validation of 3 novel DNA methylation markers of prostate cancer prognosis. J Urol. 2007;177:1753–8. [PubMed: 17437806]
59. Wang J, Syrett CM, Kramer MC, Basu A, Atchison ML, Anguera MC. Unusual maintenance of X chromosome inactivation predisposes female lymphocytes for increased expression from the inactive X. Proc Natl Acad Sci U S A. 2016;113:E2029–38. [PubMed: 27001848]
60. Walecki M, Eisel F, Klug J, et al. Androgen receptor modulates Foxp3 expression in CD4+CD25+Foxp3+ regulatory T-cells. Mol Biol Cell. 2015;26:2845–57. [PubMed: 26063731]

61. Lan Y1, Tang XS, Qin J, et al. Association of transcription factor FOXP3 gene polymorphism with genetic susceptibility to systematic lupus erythematosus in Guangxi Zhuang population. Zhonghua Yi Xue Yi Chuan Xue Za Zhi. 2010;27:433–6. [PubMed: 20677152]

62. Wu ZG, You ZS, Zhang C, et al. Association between functional polymorphisms of Foxp3 gene and the occurrence of unexplained recurrent spontaneous abortion in a Chinese Han population. Clin Dev Immunol. 2012;896458. [PubMed: 21876709]

63. Yang Q, Chen Y, Yong W. FOXP3 genetic variant and risk of acute coronary syndrome in Chinese Han population. Cell Biochem Funct. 2013;31:599–602. [PubMed: 23299803]

64. Jahan P, Cheruvu R, Tippisetty S, et al. Association of FOXP3 (rs3761548) promoter polymorphism with nondermatomal vitiligo: a study from India. J Am Acad Dermatol. 2013;69:262–6. [PubMed: 23498308]

65. Jafarzadeh A, Jamali M, Mahdavi R, et al. Circulating levels of interleukin-35 in patients with multiple sclerosis: evaluation of the influences of FOXP3 gene polymorphism and treatment program. J Mol Neurosci. 2015;55:891–7. [PubMed: 25326790]

66. Gholami M, Esfandiary A, Vatanparast M, Mirfakhraie R, Hosseini MM, Ghafouri-Fard S. Genetic variants and expression study of FOXP3 gene in acute coronary syndrome in Iranian patients. Cell Biochem Funct. 2016;34:158–62. [PubMed: 26931655]

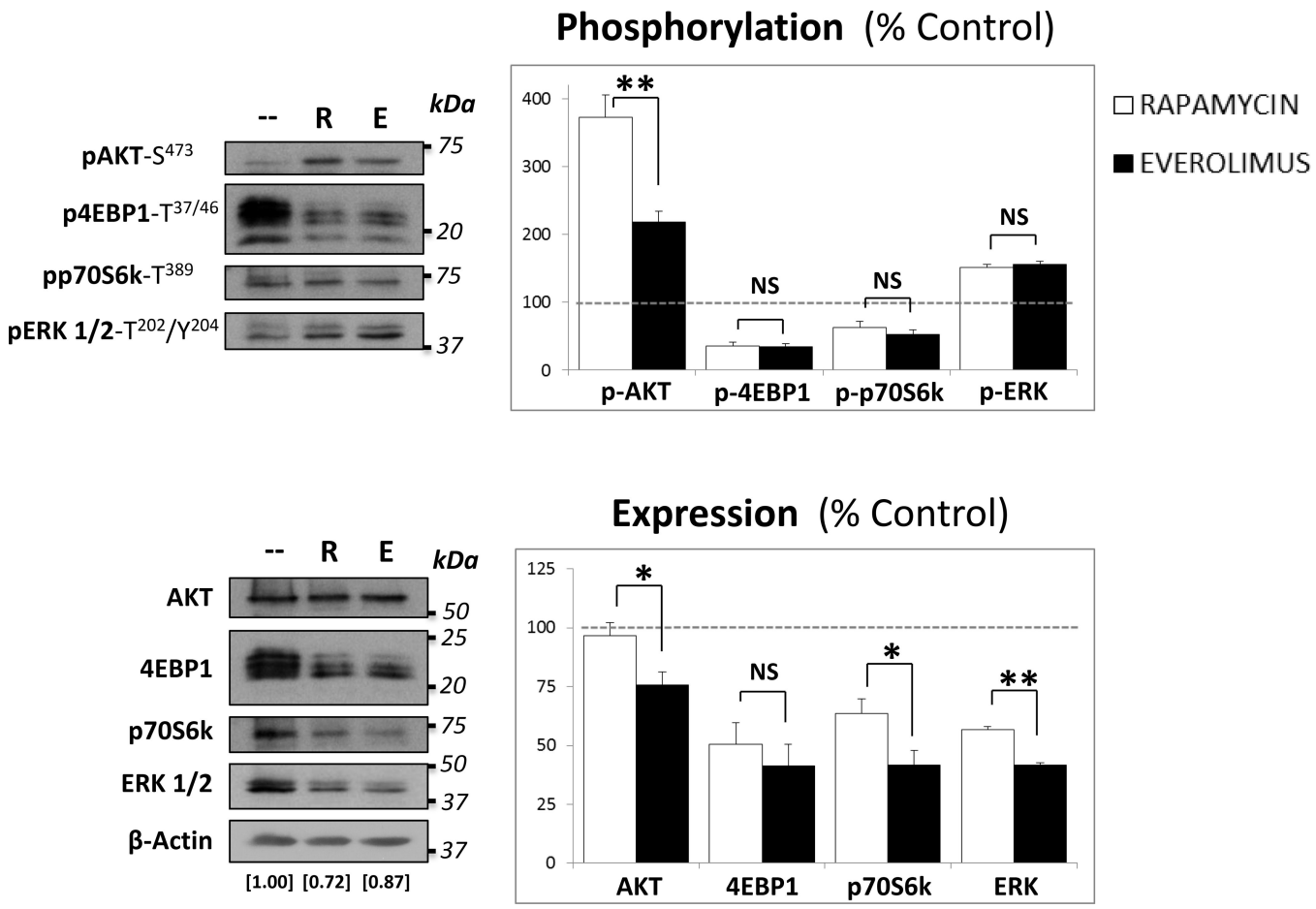

Figure 1. Effect of rapamycin and everolimus on the expression of AKT/mTOR signaling proteins in Treg cells.

Cells were expanded in Treg expansion medium either alone or with the addition of 100nM of either RAPA (R) or EVR (E). After 5 days, lysates from 10^6 Treg cells were subjected to western blot analysis to determine the levels of phosphorylated (TOP) and total (BOTTOM) expression of the mTORC2 substrate AKT, the mTORC1 substrates 4EBP1 and p70S6k, and ERK. β-actin expression was used to normalize the loaded protein levels in each line (indexes indicated as numerical values at the corresponding line in the bottom panel) of both phosphorylated and total protein blots. Right panels illustrate the average ± SD of band relative densities pooled from three different experiments *(n=3)* and shown as percentage of individual protein expression (phosphorylated -TOP- and total –BOTTOM-) relative to untreated-control cells (leveled at 100 and depicted as a dashed line). *p<0.05 and **p<0.001 indicate significant difference between RAPA and EVR-treated cells as determined by *Wilcoxon's rank sum* test. NS indicate no significant differences between both treatments.

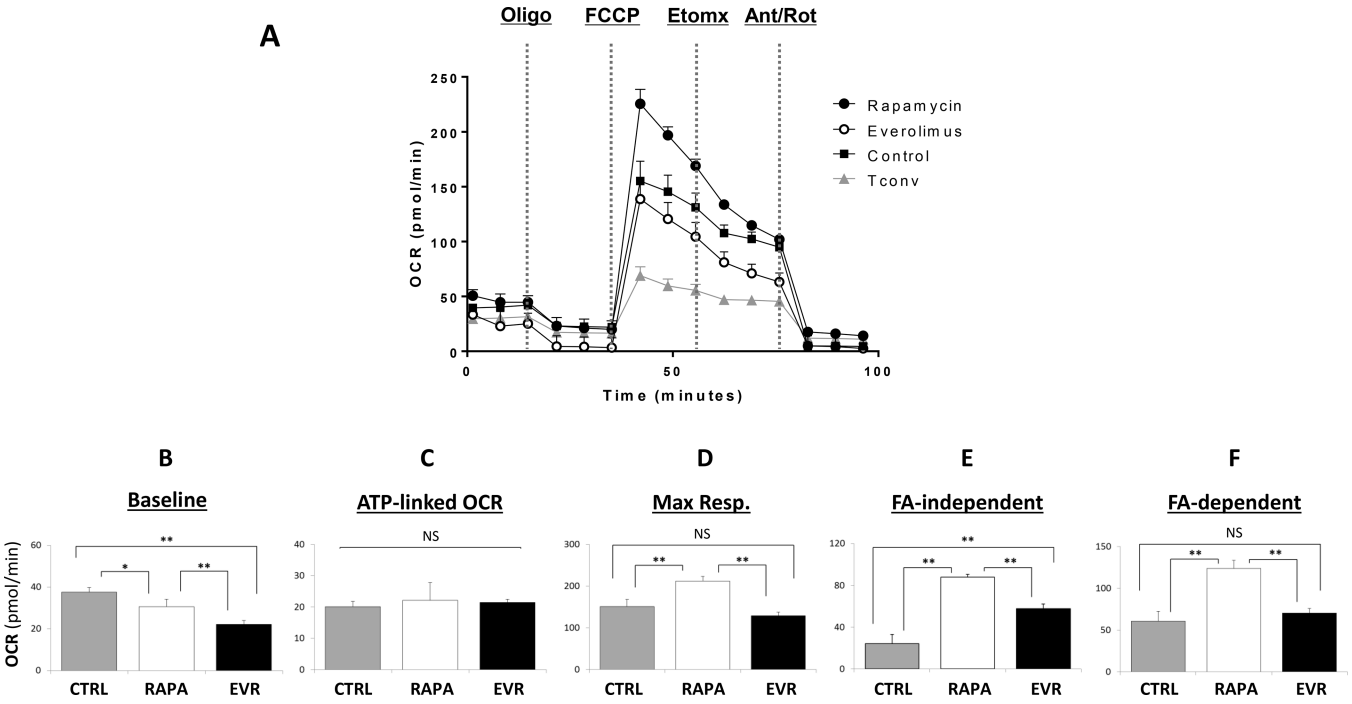

Figure 2. Effect of rapamycin and everolimus on the oxygen consumption rates of Treg cells.

(A) Oxygen Consumption Rates (OCR, pMoles/min) were measured in 5 day-expanded Treg cells in the presence of 100nM of rapamycin (closed circles) or everolimus (open circles). The results were compared with the profile generated with untreated Treg cells (Control, closed squares) and conventional T cells (Tconv, closed triangles) cultured in the same Treg cell expansion medium for 5 days. **(B-F)** The OCR parameters were generated from a modification of the Seahorse XF Mito Stress Test Report Generator detailed in SDC, Material and Methods, and are shown as follows: (B) Baseline OCR, (C) ATP-linked oxygen consumption, (D) Maximal respiratory capacity -Max. Resp.-, (E) (F) non fatty acid oxidation-driven capacity -FA-independent-, and (E) endogenous fatty acid oxidation-driven capacity -FA-dependent.-, ().-, Data represents the mean ± SD pooled from at least three independent *(n=3)* experiments and five replicates per condition in each experiment. *p<0.05 and **p<0.001 indicate significant differences as measured by Kruskal–Wallis ANOVA followed by post-hoc Wilcoxon test to assess treatment-specific differences. NS indicate no significant differences.

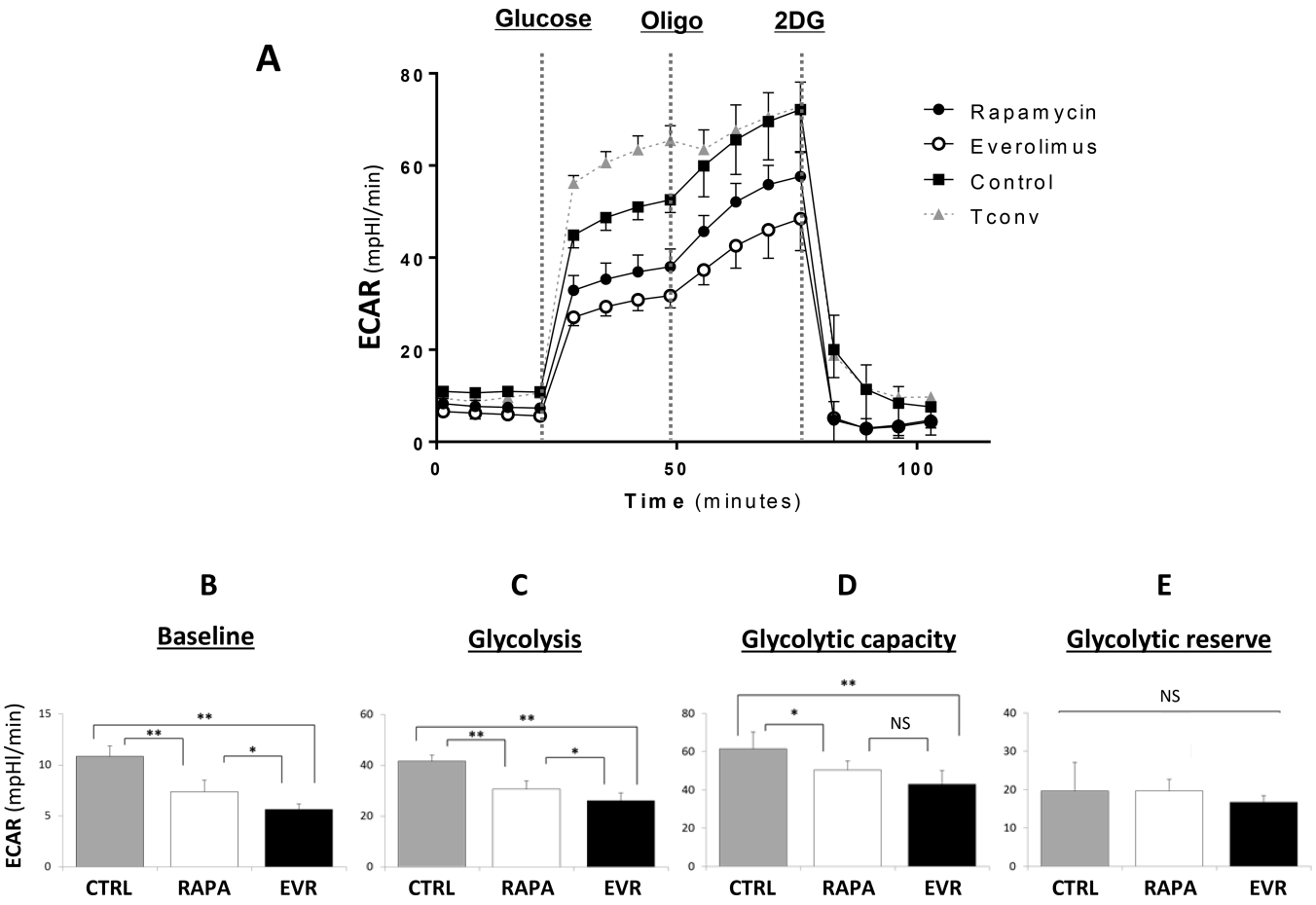

Figure 3. Effect of rapamycin and everolimus on the extracellular acidification rates of Treg cells.

(A) The extracellular acidification rates (ECAR, mpH/min) were measured in Treg cells expanded 5 days in the presence of 100nM of rapamycin (closed circles) or everolimus (open circles), and compared with 5 day-expanded untreated Treg cells (Control, closed squares) and conventional T cells (Tconv, closed triangles) cultured in the same Treg cell expansion medium. **(B-E)** The ECAR parameters were generated with the Seahorse XF Glycolysis Stress Test Report Generator and are shown as follows: (B) Baseline ECAR, (C) Glycolysis, (D) Maximal glycolytic capacity -Glycol. Capacity-, and (E) Glycolytic reserve -Glycol. Reserve-. Data is showing as the mean ± SD pooled from at least three independent (*n=3*) experiments and five replicates per condition in each experiment. *p<0.05 and **p<0.001 indicate significant pairwise differences in Wilcoxon test following Kruskal–Wallis ANOVA test. NS indicate no significant differences among treatments.

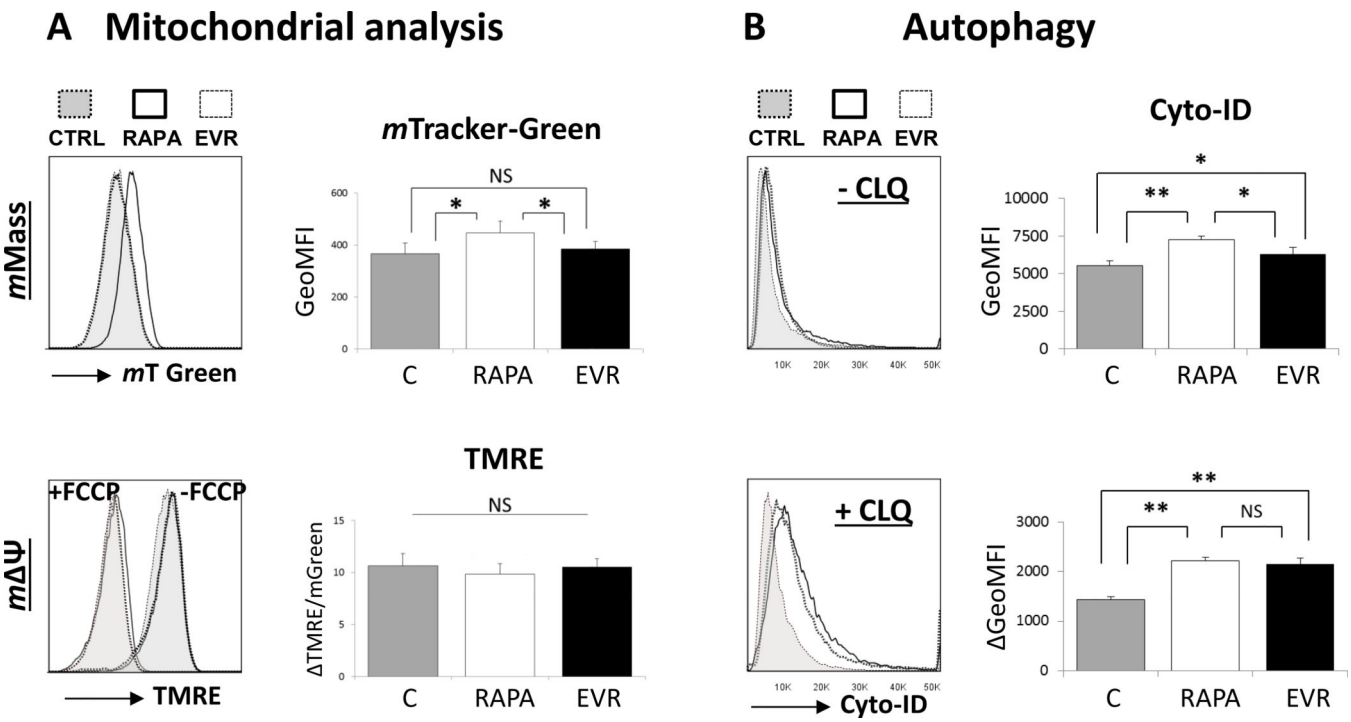

Figure 4.

Effect of rapamycin and everolimus on the mitochondrial integrity and autophagy in Treg cells were measured by flow cytometry analysis. Histograms (left) are representative single individual experiments of the corresponding bar-graphs (right) depicting the pooled (n=6) average mean fluorescence intensity (MFI)± SD from 5-day untreated (CTRL), 100nM rapamycin-treated (RAPA), or 100nM everolimus-treated (EVR) expanded Treg cells. **(A)** Mitochondrial mass (TOP) was measured with MitoTracker Green, which is independent from the mitochondrial membrane potential ($m\Delta\Psi$). (BOTTOM) Changes in $m\Delta\Psi$ were analyzed by flow cytometry with the fluorescent probe TMRE. The resulting MFI within cells treated only with TMRE was corrected from the corresponding MFI of cells pre-treated with FCCP. Results for each condition are shown as the rate between TMRE increments (±FCCP) and the corresponding MitoTracker Green value, which normalize $m\Delta\Psi$ per equal mitochondrial mass. **(B)** The measurements of autophagic vacuole formation (TOP) were performed with the Cyto-ID autophagy detection kit. The accumulation of autophagosomes after the addition of the autophagic inhibitor Chloroquine (CLQ) for 6 hours before the addition of Cyto-ID Green solution was used to determine the autophagic flux (BOTTOM). The autophagosome flux is shown as the average MFI mean fluorescence intensity increase in cells pre-treated with CLQ compared to the cells in the absence of CLQ. Statistical differences among treatments were tested by Kruskal–Wallis ANOVA followed by post-hoc Wilcoxon test to assess treatment-specific differences. *p<0.05 and **p<0. 001 indicate significant pairwise differences; NS, no significant differences.

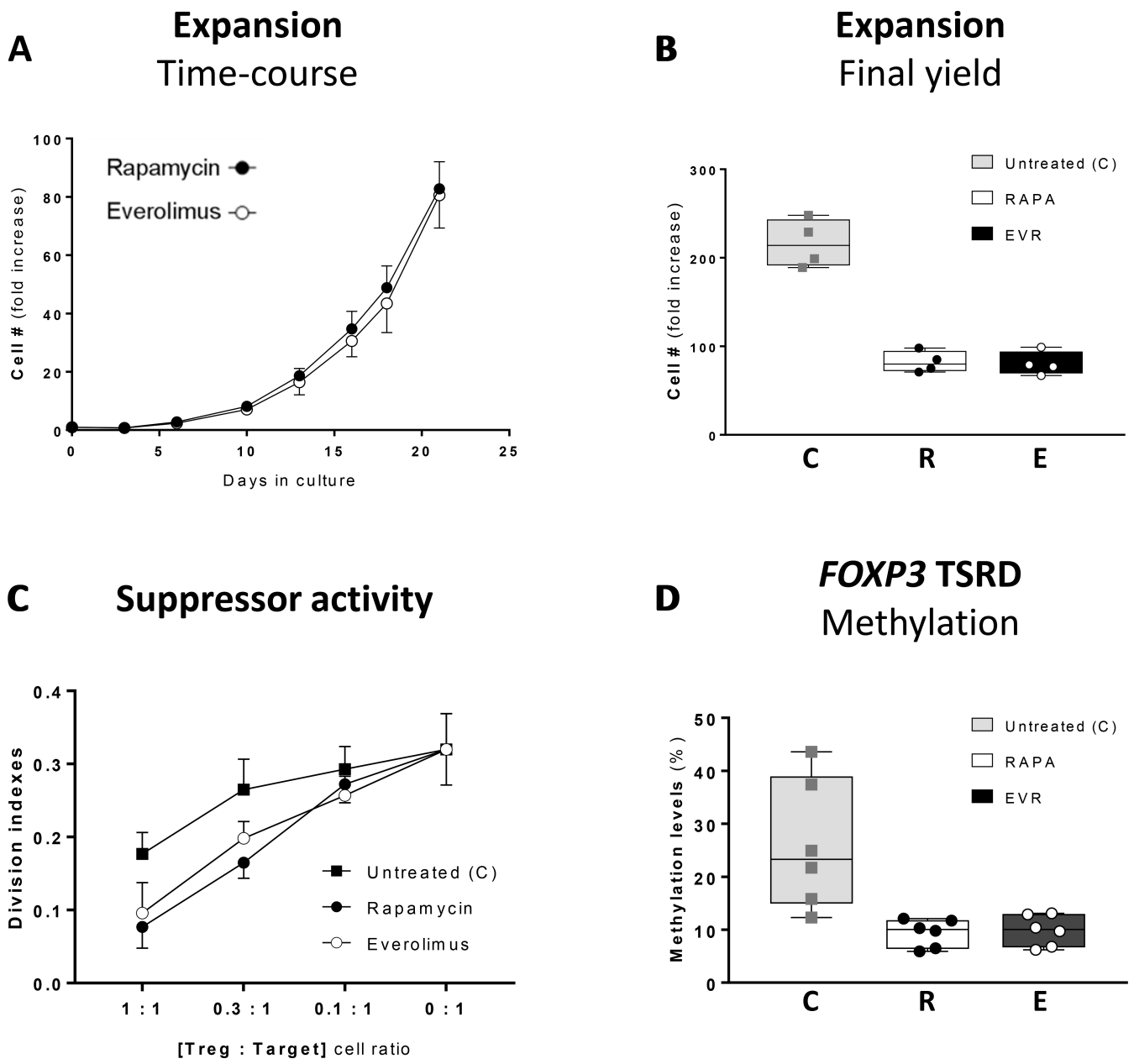

Figure 5. Long-term effect of rapamycin and everolimus on the expansion, *FOXP3* TSDR methylation, suppressor function and phenotype of Treg cells.

$CD4^+CD25^+$ cells were expanded in Treg expansion medium in the presence of 100nM RAPA or 100 nM EVR for 21 days. (**A**) Cell numbers for RAPA (closed circles) or EVR (empty circles)-treated cells were quantified every 2–4 days. The plot illustrates the temporal fold increase in cell numbers with respect to the initial seeding. (**B**) Cell yield corresponding to the 21-day expansion in untreated (C), RAPA-treated (R), or EVR-treated (E) cells shown as interquartile (25/75) range box-and-whiskers plots with median and individual values of n=4 measurements. (**C**) Suppressive activity induced in allogeneic CFSE-labeled responder T cells in co-culture for 72 hours with different of Treg:Target labeled cell ratios. Suppressor activity was measured by the decrease of division indexes in the CFSE-labeled target cells.

(**D**) Methylation status (as percentage) of the TSDR *FOXP3* in untreated (C), RAPA-treated (R), or EVR-treated (E) cells is shown as interquartile range box-and-whiskers plots with median and individual values of n=6 measurements.

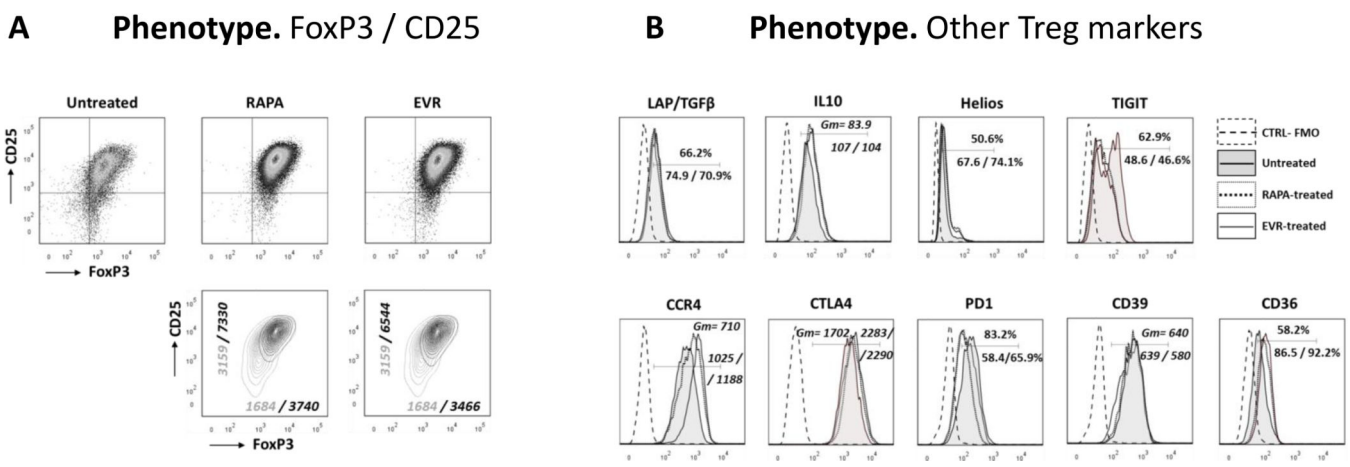

Figure 6. Long-term effect of rapamycin and everolimus on the phenotype of Treg cells.

Representative phenotype analysis of 21-day expanded CD4+/FoxP3+/CD25+ population (**A**) Top dot-plots represent the expression of FoxP3 and CD25 in cell cultures in the absence (Control) or in the presence of RAPA or EVR. Bottom panels depict CD25/FoxP3 countour plots of untreated (grey lines) overlaid with treated (black) cells. The corresponding GeoMean Fluorescence Intensities of FoxP3 and CD25 are indicated inside the panels (grey: untreated / black: treated). (**B**) Histogram plots comparing the expression profiles of different proteins in untreated (shaded), RAPA-treated (dotted line) and EVR-treated (solid line) cells. These proteins are differentially expressed in Tregs and Tconv cells (see Figure S7 in SDC). The expression levels of the different proteins are indicated inside the panels as GeoMean Fluorescence Intensities (Gm) or as percentages of positive cells for untreated, RAPA-treated and EVR-treated cells (first / second / third value, respectively). FMO controls are depicted as dashed lines. This is a representative of 3 different experiments.

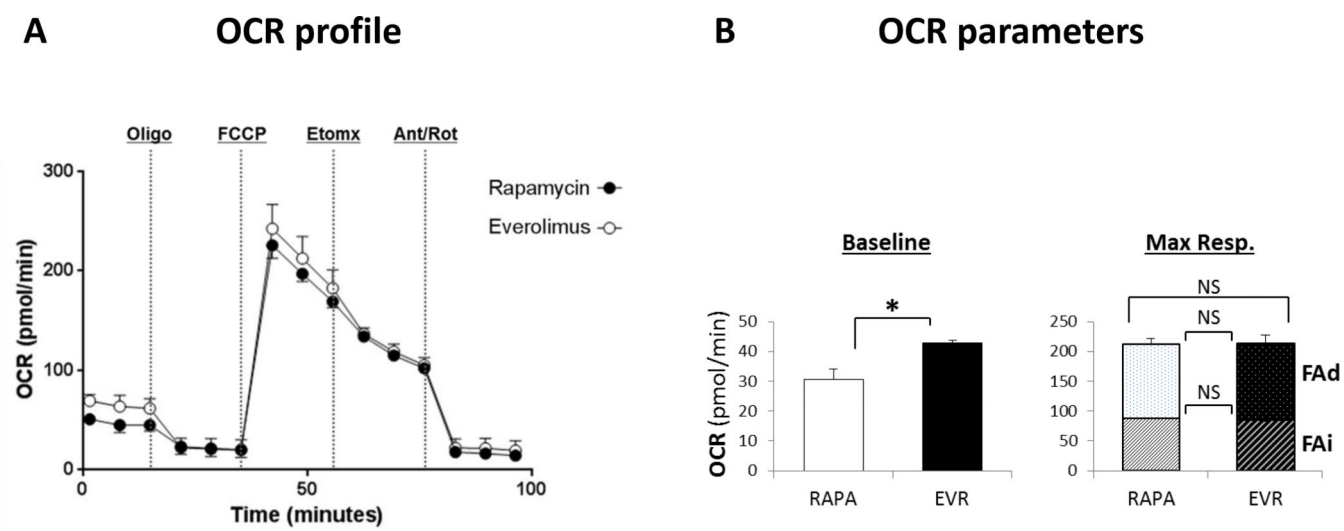

Figure 7. Long-term effect of rapamycin and everolimus on oxygen consumption rates of Treg cells.

(**A**) The same CD4+CD25+ cells expanded in Treg expansion medium in the presence of 100nM RAPA (closed circles) or 100 nM EVR (empty circles) for 21 days depicted in Figure 5A were used to analyze the oxygen consumption rate (OCR), as in Figure 2. (**B**) Baseline OCR and maximal respiratory capacity (Max. Resp.) levels for RAPA- and EVR-treated cells were generated as in Figure 2. Fatty acid-dependent (FAd) and fatty acid-independent (FAi) rates are shown as stacked columns in Max. Resp. (*) indicates a significant ($p<0.05$) difference between RAPA and EVR treatments as measured by *Wilcoxon's rank sum* test out of 4 independent experiments and five replicates per condition in each experiment; NS, not significant difference